Available online at www.sciencedirect.com
ScienceDirect
Ceramics International 34 (2008) 1207–1213
CERAMICS INTERNATIONAL
www.elsevier.com/locate/ceramint

Sintering of clay-chamotte ceramic composites for refractory bricks

C.N. Djangang [a,b,c], A. Elimbi [a], U.C. Melo [a,c], G.L. Lecomte [b], C. Nkoumbou [d], J. Soro [b], J.P. Bonnet [b], P. Blanchart [b,*], D. Njopwouo [a]

[a] *Laboratory of Physico-Chemistry of Mineral Materials, University of Yaounde I, P.O. Box. 812, Yaounde, Cameroon*
[b] *GEMH, ENSCI 47-73, Avenue Albert Thomas 87065 Limoges, France*
[c] *Local Material Promotion Authority (MIPROMALO), P.O. Box. 2396 Yaounde, Cameroon*
[d] *Department of Earth Sciences, Faculty of Science, University of Yaounde I, P.O. Box. 812, Yaounde, Cameroon*

Received 21 November 2006; received in revised form 7 February 2007; accepted 28 February 2007
Available online 20 April 2007

Abstract

Clay-chamotte composites were realized for manufacturing refractory bricks. We used two kaolinitic refractory clays mined in Cameroon and two calcined clays (chamottes) with a large grain size (0.1–4 mm). Clay-chamotte composites containing various quantities of chamotte (0–50 wt%) were shaped and sintered at 1200–1350 °C. The structural characteristics of composites indicated the presence of quartz from the initial clay, cristobalite and mullite. SEM observations revealed very heterogeneous microstructures where porosity is weakly distributed and large pores are entrapped at the vicinity of large chamotte and quartz grains. In general, the global porosity increases with the chamotte content. A specific interpretation of the matrix role on the global sintering behaviour reveals that only a part of the matrix acts effectively. Since the most part of the global porosity is within the matrix, it is distributed in matrix zones, which participate effectively to sintering and in inert matrix zones where larger pores occur. The global mechanical strength is controlled by the matrix behaviour, but the high porosity of this phase is unfavourable to high strength values. Besides, the occurrence of larges pores and local cracks at large grain interfaces from thermal stresses are critical flaws, which reduce the mechanical strength.

Keywords: A. Sintering; D. Clays; Refractory; Chamotte; Cameroon

1. Introduction

Ceramic composite are often designed for the development of structural ceramics which microstructural heterogeneity is an important behaviour for the optimisation of the global properties [1,2]. Heterogeneities are related to the physico-chemical and structural particularities of initial powders, to the grains size repartition and shape as well as to the individual transformation and interactions of components during the sintering process. In general, initial compositions are selected to attain the desired performance of final products. In the case of refractory materials, porosity and mechanical strength are important parameters, which depend on the individual sintering behaviour of phases, but with the interactions between phases at high temperature.

Common refractory materials containing refractory clays are porous ceramic based on the mixture of plastic clays (with kaolinite as main clay mineral) and non-plastic raw materials such as chamotte and quartz. Chamotte is a preliminary fired clay above the working temperature range for the relative completion of all thermal reactions. Chamotte is mixed with clays to reduce the sintering stresses such as local cracks and flaws [3–5].

Kaolinite chemical, physical and structural transformations have been extensively reviewed in the literature, emphasizing the effect of heating conditions on final properties and microstructural aspects [6–13]. It points to the control of a large range of parameters during the firing of sintering materials (clay) in the presence of inert phase, chamotte, to obtain high quality products.

This study presents investigations on microstructural transformations that occur during the sintering of refractory clays mixed with various chamotte quantities. Clays used in this work are from Mayouom and Mvan sites in Cameroon.

* Corresponding author. Tel.: +33 555452211.
E-mail address: p_blanchart@ensci.fr (P. Blanchart).

0272-8842/$34.00
doi:10.1016/j.ceramint.2007.02.012

Characterisations include the elaboration of samples, the measurement of their physical properties (porosity and flexural strength), structural and the microstructural characterization by XRD and by SEM observations. The influence of phases size and quantities on microstructural characteristics are related to the densification behaviour during firing and to the mechanical properties of fired materials.

2. Materials and techniques

Two samples of clay raw materials from quarries in Cameroon were used. They are the MY38 from the large deposit of Mayouom clay at Foumban (08°51′N; 10° 59′E; West Province) and the BEAC from Mvan near Yaoundé (03°50′N; 11°32′E; Centre Province). Clays were used as crude raw clays in compositions and also after firing at 1350 °C to form chamottes. Chamotte agglomerates were crushed and sieved at controlled size by mixing 33 wt% of the 1–4 mm fraction (Gaussian average 3.1 mm) and 67 wt% of 0.1–1 mm fraction (Gaussian average 0.51 mm). The finer fraction below 0.1 mm was removed. CHM and CHB designate chamottes from MY38 and BEAC, respectively, and their characteristics are in Table 1.

The mineralogical composition of MY38 clay contains phyllosilicate minerals, mostly kaolinite and small quantity of illite (Table 2). The average size of these minerals (2.1 μm) is similar to that of phyllosilicates in common clays. Associated non-clay minerals are quartz and a minor quantity of anatase. BEAC composition is similar except in the quartz content which is higher, giving rise a lower plasticity in comparison to that of MY38 (plasticity index 16 and 20, respectively). The size of the quartz fraction above 5 μm was measured after separation from phyllosilicates. Average size are 10.6 μm for MY38 and 47.5 μm for BEAC. In this clay, very large grains (up to 1 mm) highly increase the average size.

During firing, the MY38 clay and the BEAC pure clay fraction exhibit a high shrinkage, which induces cracks in products and reduces drastically the mechanical strength. It can be minimized by mixing with clays a significant amount of chamotte, typically 10–50 wt%. In this study, we investigated two compositional domains: MY38 clay with 30–50 wt% of CHM chamotte; BEAC clay mixed with 10–30 wt% of CHB chamotte. The lower chamotte content in the mixture containing BEAC is due to the reduced shrinkage during firing from the higher amount of quartz.

Samples were realized following the various steps indicated in the flow chart of Fig. 1. With MY38 clay, compositions contain 30, 40 and 50 wt% of CHM. With the sandy BEAC clay, compositions contain 0, 10, 20 and 30 wt% of CHB. Water was added, to form plastic pastes with a moisture content between 16 and 22 wt%. Plastic pastes were shaped by unidirectional pressing at 2.5 MPa. After drying at room temperature (48 h) and at 50 °C (10 h) and 110 °C (10 h), bricks were fired in an electrical kiln under air at 1200, 1250, 1300 and 1350 °C. The heating rate was 3 °C/min and the dwell time at the peak temperatures was 4 h. Processing techniques and thermal cycles are very similar to that used by small industries in Cameroon, that ensures a technology transfer.

Table 1
Characteristics of chamottes

Chamottes	Major minerals	Minor minerals	Granulometry (%)	
			4–1 mm	1–0.1 mm
CHM	Mullite, Cristobalite	Quartz, rutile	33	67
CHB	Mullite, Cristobalite, quartz	Rutile	33	67

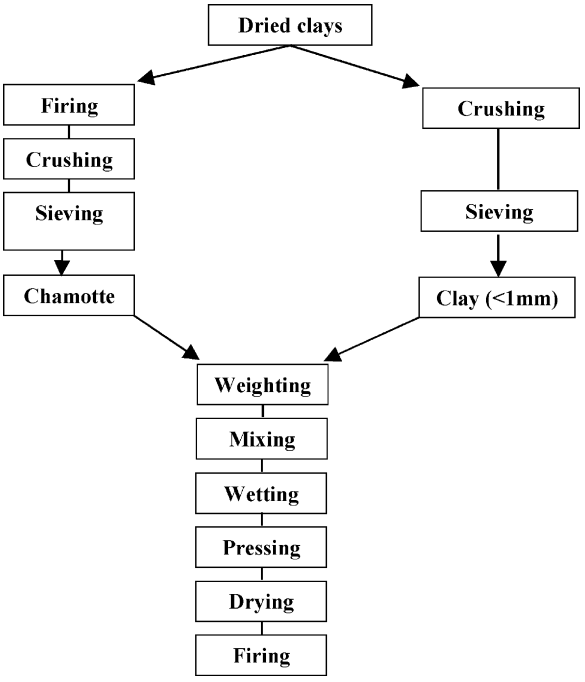

Fig. 1. Schematic representation of the process technology.

With sintered bricks, we characterized the bulk density, the open porosity by the Archimedes method and the flexural strength (J.J. instrument) using a three points bending system.

SEM observations of various fired materials were made on polished section (Hitachi S-2500) and structural analyses of grounded materials were by X-ray diffraction (Inel CPS-120). The sintering behaviour was characterized by thermo-mechanical analyses up to 1300 °C (DI24 Adamel instrument).

Table 2
Mineralogical and particle size distributions of clays

	Kaolinite	Illite	Quartz (α)	Anatase	Goethite	Ilmenite	Particles <63 μm (%)
MY38	82.3	8	2.9	4	0.9	–	98
BEAC	67.3	2.3	27.2	0.5	–	2.1	50

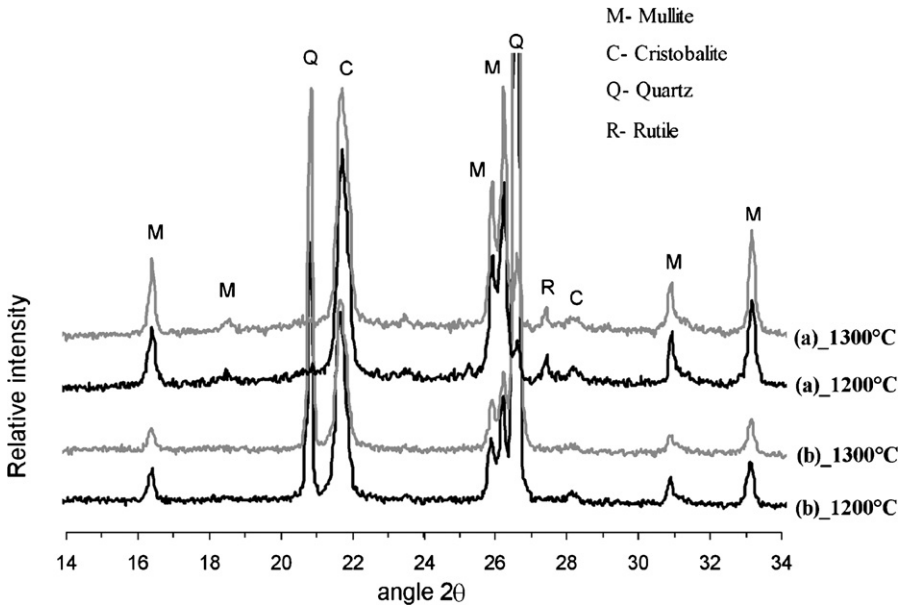

Fig. 2. XRD patterns of fired of bricks from mixture: (a) 50 wt% MY38 + 50 wt% CHM; (b) 80 wt% BEAC + 20 wt% CHB.

3. Results and discussion

3.1. Structural and microstructural characteristics of materials

The crystalline phases identified by XRD in both MY38 and BEAC, are mullite, quartz, cristobalite and rutile (Fig. 2). But differences are evidenced in MY38, since the mullite content is higher and the quartz content is lower. The high quartz initial content in BEAC, which size is large, limits the quartz interaction with the surrounding silico-aluminate phases. The quartz cristobalite transformation is effective, but mainly in MY38, where the grain size of initial quartz is small. For the two materials, the temperature increase from 1200 to 1300 °C does not favours this transformation, which proves that materials attain a steady state at 1200 °C and above. Moreover, MY38 background patterns (Fig. 2) show a slight positive variation from the presence of amorphous phases. It could be remaining amorphous phases or vitreous phases from melted phases at high temperature. These phases favour the creep of products under constant load at high temperature.

The microstructure of MY38 (50 wt% of CHM) and BEAC (20 wt% of CHB) samples sintered at 1200 °C are presented in Fig. 3a and b, respectively. In these photos, the heterogeneous character of microstructure can be seen very clearly. Within the fine grain matrix phase, we observe very large grains of chamotte in MY38 and chamotte and quartz in BEAC. In the latter sample, large quartz grains can't be easily distinguished from chamotte grains but observations using optical microscopy revealed their homogeneous distribution. In the matrix phase, entrapped pores can't be distinguished due to their small size in comparison to the used scale. However, few sintering defects are detected in both materials, and the presence of such defects is observed in all compacts whatever the chamotte content. Defects are large size elongated pores along the biggest grains whose existence is supposed to be favoured by the differential densification during sintering between chamotte and matrix (Fig. 3c). Besides, differential dilatations of large quartz grains during cooling induce elongated cracks along grain boundaries as is shown in the detailed photo of Fig. 3d. It is evidenced that both elongated pores and interfacial cracks lead to the lowering of mechanical properties.

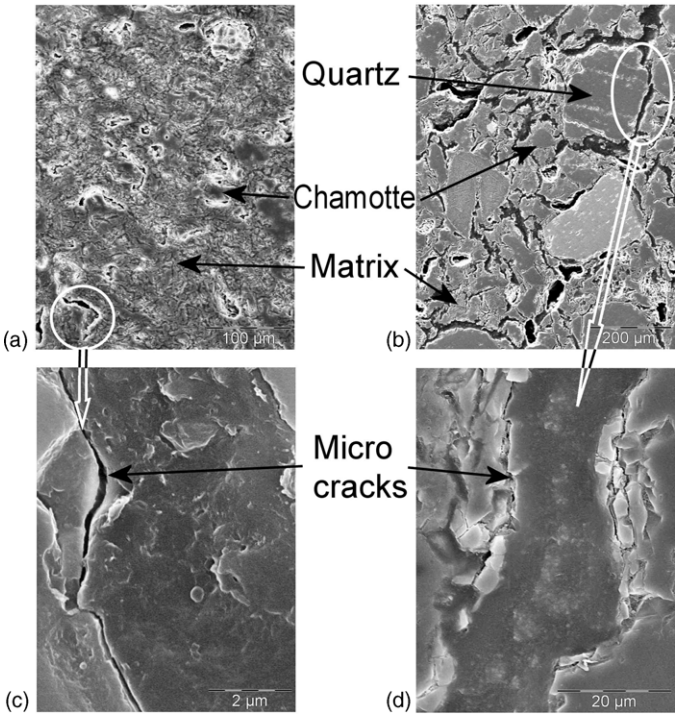

Fig. 3. Microstructure of bricks fired at 1200 °C: (a) 50 wt% MY38 + 50 wt% CHM, (b) 80 wt% BEAC + 20 wt% CHB. Microcracks along interfaces between matrix and grain of chamotte (c) and quartz (d).

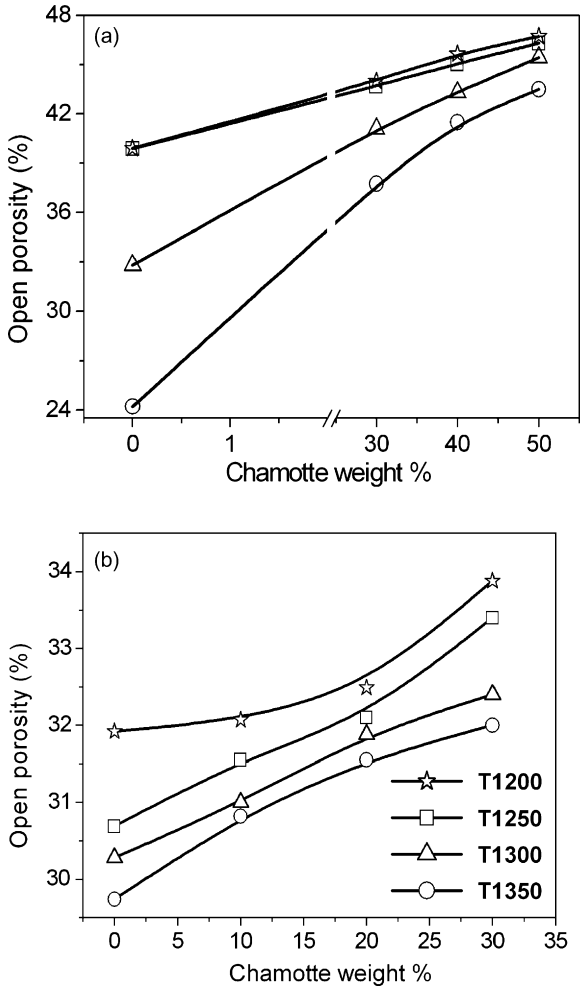

Fig. 4. Open porosity at different firing temperatures as a function of chamotte quantity with MY38 (a); BEAC (b).

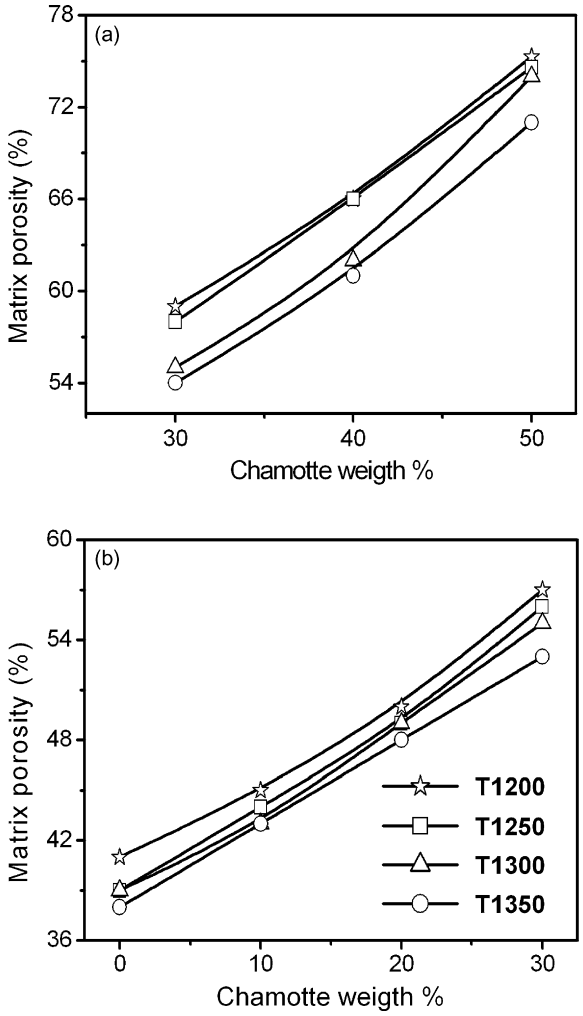

Fig. 5. Matrix porosity at different firing temperatures as a function of chamotte quantity with MY38 (a); BEAC (b).

3.2. Characteristics of sintered materials

Fig. 4a and b show the global open porosity at temperatures from 1200 to 1350 °C as function of the chamotte content in the initial formulation. For a given temperature, the open porosity increases with the added chamotte quantity but is reduced when the firing temperature changes from 1200 to 1350 °C. In the used temperature range it is supposed that chamotte does not undergo any shrinkage since it was preliminary fired at 1350 °C and that the global shrinkage is controlled by restricted zones in the matrix phase. In initial mixtures, the matrix phase is a plastic clay added during a wet mixing process and discontinuities in the stacking of clay plates promote an additional porosity. Particularly, the clay particles are oriented and preferentially packed tangentially to non-plastic particles (chamotte and quartz) [14,15]. During firing both the difference in porosity between the clay matrix and chamotte particles as well as the preferential stacking of clay platelets leads to a differential shrinkage with an entrapped porosity.

From Fig. 4a and b we also observe a very different densification behaviour, since the porosity of BEAC fired clay is significantly lower than that of fired MY38. A specific role of the clay mineral fractions in both clays is not supposed to have an important role since they present very similar mineralogical and chemical characteristics (Tables 2 and 3). We suppose that the quantity and size repartition of quartz fraction in BEAC favour a more compact packing during the compaction process, which favours the densification during sintering [16]. The same tendency is observed when chamotte is mixed to both clays, since porosity evolves slightly with BEAC whereas it changes significantly for MY38.

Table 3
Chemical compositions of clays

	SiO_2	Al_2O_3	Fe_2O_3	MnO	MgO	CaO	Na_2O	K_2O	TiO_2	P_2O_5	L.O.I.
MY38	44.81	35.80	0.79	<0.01	<0.01	<0.01	<0.01	0.94	3.96	0.37	13.28
BEAC	60.02	27.83	2.17	<0.01	0.56	0.08	0.22	0.39	1.55	0.02	7.08

The temperature influence is more effective with MY38 based material which mineralogical composition contains 8 wt% of illite mineral. It enhances the densification by the formation of a liquid phase, in accordance with the ternary SiO_2–Al_2O_3–K_2O system [17–18]. For both materials, the global shrinkage is mainly governed by the behaviour of the finer fraction in the matrix phase.

Fig. 5a and b shows the matrix open porosity as a function of the chamotte content and temperature, using data of Fig. 4a and b and corrected with the quartz fraction in Table 2. Note that the open porosity of the sintered clay matrix increases strongly with increasing the inclusion quantities and exceeds significantly the global porosity. BEAC favours a lower porosity of the matrix in comparison to MY38 and this is related to differences in mineralogical compositions discussed above. In general the relationship between density and mechanical strength is well described by the following relation [19]:

$$\sigma = \sigma_o \exp(-nP) \quad (1)$$

where σ_o is the strength of a perfectly dense material and P is the porosity vol.%. n is a parameter related to the microstructure type (4–7). For our material, the high P values (35–75 vol.%) in the matrix are in a curve region where both the strength and the strength variation are low, which results in the low global strength for all materials.

The variation of matrix densities proves that the presence of non-sinterable inclusions decreases the local density between large grains. It also creates thermal stresses during the high temperature sintering process due to differential shrinkages and results in large relative deformations between adjacent phases. Particularly, if stresses become large enough at the interfaces having a low fracture toughness, crack formation occurs which cannot be consolidated during the thermal cycle (Fig. 3c and d). Correspondingly, flexural strengths are below 6 MPa and their variation with the chamotte content and temperature (Fig. 6a and b) are limited. Particularly for BEAC material, a high chamotte content decreases the strength. Since strength does not exceed 2 MPa, the role of supplementary internal stresses at large quartz interfaces is pointed out.

3.3. Sintering of materials

The densification behaviour as a function of time and temperature up to 1300 °C are presented in Fig. 7a for MY38 with 0, 30 and 50 wt% of CHM. In Fig. 7b, the densification rates for the same compositions are plotted against time and temperature. Similarly in Fig. 8a and b, sintering plots and

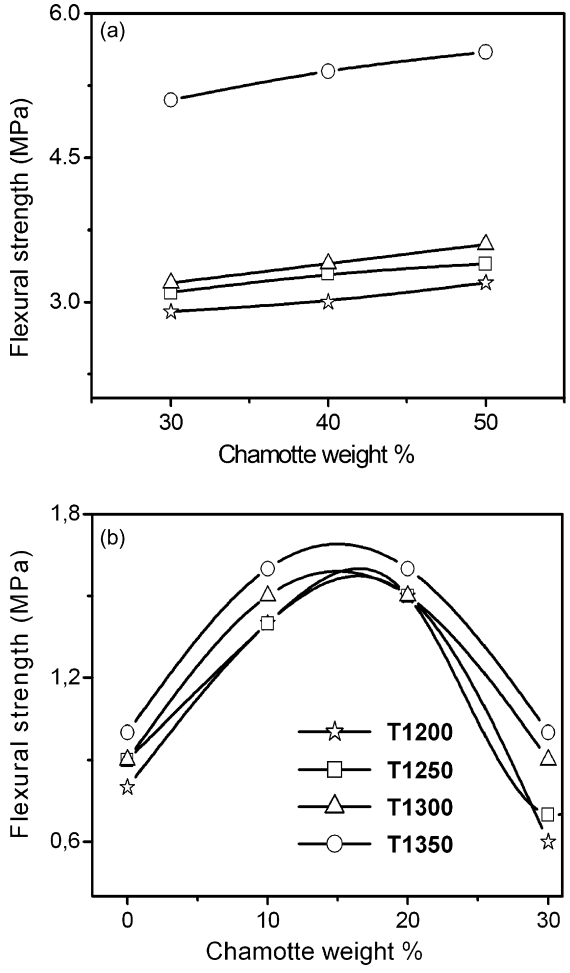

Fig. 6. Flexural strength at different firing temperatures as a function of chamotte quantity with MY38 (a); BEAC (b).

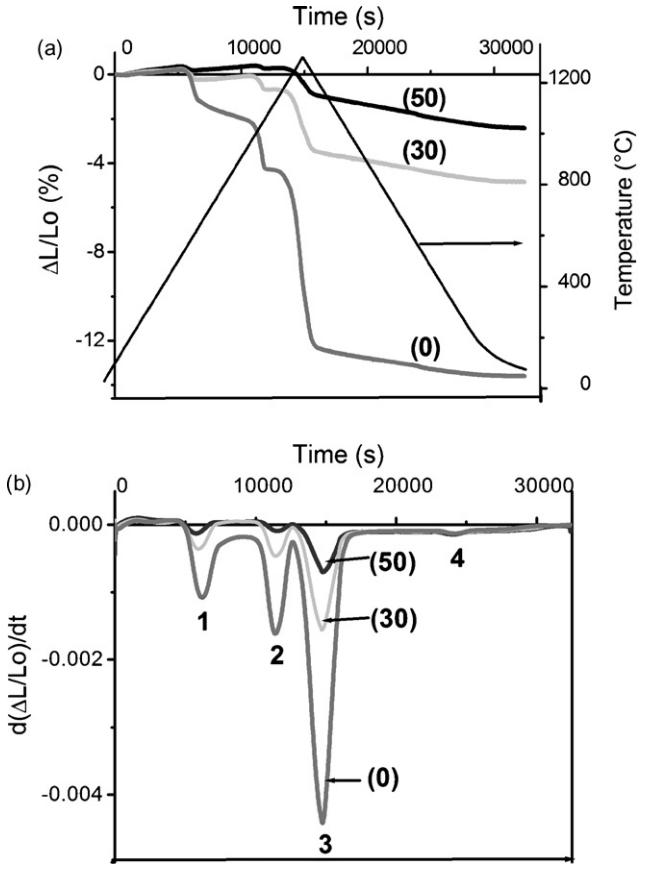

Fig. 7. (a) Sintering curves of clay-chamotte mixture, (0) 100 wt% MY38, (30) 70 wt% MY38 + 30 wt% CHM, (50) 50 wt% MY38 + 50 wt% CHM. (b) Densification rates; peak 1 dehydroxylation; peak 2 structural reorganization, peak 3 main densification; peak 4 β to α quartz transformation.

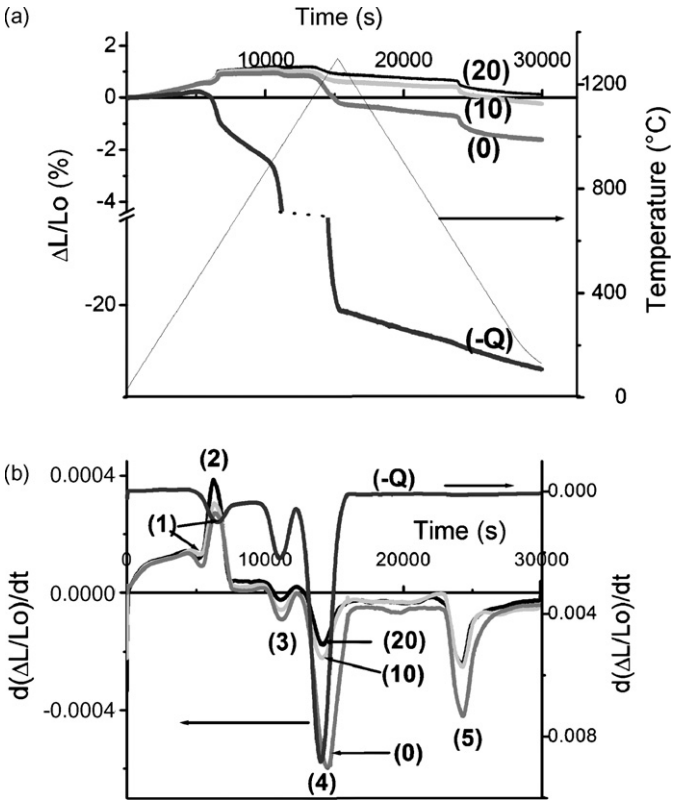

Fig. 8. (a) Sintering curves of clay-chamotte mixture, (0) 100 wt% BEAC, (10) 90 wt% BEAC + 10 wt% CHB, (20) 80 wt% BEAC + 20 wt% CHB, (-Q) 100 wt% BEAC (fraction <15 μm). (b) Densification rates; peak 1 dehydroxylation; peak 2 α to β quartz transformation, peak 3 structural reorganization, peak 4 main densification, peak 5 β to α quartz transformation.

densification rates for BEAC with 0, 20 and 30 wt% of CHB are presented.

In all curves, densification rates are highly increased within the following temperature intervals: 500–650, 950–1020 and 1050–1300 °C. They are attributed, respectively, to the dehydroxylation of clay minerals, to the structural reorganisation of dehydroxylated clays mineral and to the sintering process itself. During the last densification stage, both transformations of clay minerals to silico-aluminate phases and interaction between phases occur. During cooling, a specific variation is seen at 573 °C, which is the β to α quartz transformation. For both clays, when the chamotte content increases, densification values are reduced, but peak positions of densification rates occur at similar time and temperature ranges (Figs. 7b and 8b). It means that densification is originated from the matrix material and that no interaction between clay and chamotte or quartz occurs. The behaviour of BEAC differs from that of MY38 since it contains large quartz grains (27 wt% in Table 2). They act as a supplementary grain phase with very limited morphological transformations, although some cristobalite is seen in XRD patterns of Fig. 2. Their role on sintering is evidenced on the additional curve of Fig. 7, where the sintering curve of the fine clay fraction (<15 μm) is presented. The higher value of densification points to the role of large quartz grains on densification.

The sintering of granular composites is mainly governed by the shrinkage of the matrix where porosity is distributed. From Fig. 5a and b, it is interesting to note that the matrix porosity increases with the chamotte content and it can be attributed to agglomeration and textural effects from chamotte and quartz grains.

Matrix porosity P_{matrix} of Fig. 5a and b are obtained from data of Fig. 4a and b, using a simple geometrical model:

$$P_{\text{matrix}} = \frac{P_{\text{g}}}{1 - V_{\text{ch}}} \tag{2}$$

where P_{g} is the porosity of the material and V_{ch} is the chamotte volume ratio in the material. It is calculated from the weight ratio of chamotte, using the chamotte density values.

This approach considers a homogeneous repartition of the chamotte phase within a uniform matrix. Nevertheless, chamotte particles are not ideally distributed and an additional porosity within agglomerates or in restricted areas where strong interactions between neighbour chamotte grains occur. In these areas, the matrix phase doesn't contribute to the global densification and additional large porosity areas are created. Correspondingly, photos of Fig. 3a–d clearly show large pores entrapped between large grains.

The partial matrix which contributes to densification is supposed to behave the same in each composites and in the pure material. Therefore, the ratio P of the pore volume in the matrix V_{pm} to bulk material volume V_{bm} is kept constant:

$$P = \frac{V_{\text{pm}}}{V_{\text{bm}}} = \frac{P_{\text{m}}}{1 - P_{\text{m}}} \tag{3}$$

where P_{m} is the porosity of the pure matrix.

To account for the additional porosity, the volume fraction $V_{\text{S}}^{\%}$ of the matrix which effectively contributes to the global densification is [20]:

$$V_{\text{S}}^{\%} = \frac{(1 + V_{\text{ch}})(P_{\text{f}}^{\%} - P_{i}^{\%})}{P_{\text{f}}^{\text{m}} - P_{i}^{\text{m}}} \tag{4}$$

where V_{ch} is the volume ratio of the chamotte against the matrix volume. $P^{\%}$ and P^{m} are the porosity ratio in Eq. (3), for the material and the matrix themselves in the final and initial states. Results are presented in Table 4 for the two clay based

Table 4
Global porosity P_{g}, matrix porosity P_{matrix} and additional porosity $V_{\text{add}}^{\%}$

Chamotte (vol.%)	P_{g}	P_{matrix}	$V_{\text{add}}^{\%}$	$V_{\text{S}}^{\%}$
MY38				
0	33	33	0	100
30	38	55	17	68
40	43	62	19	63
50	45	73	21	59
BEAC				
0	30.5	30.5	0	100
10	31	52	25	57
20	31.8	63	27	54
30	32.2	73.5	33	46

$V_{\text{S}}^{\%}$ is the volume fraction of sintered matrix material.

materials. In the case of MY38, the matrix ratio which effectively contributes to the global densification decreases with the chamotte content. It is in accordance with the non-uniformity of chamotte grains explained above and this tendency is favoured at higher chamotte content. For BEAC, the obtained values are lower because we took into account the quartz content which behaves as a supplementary granular phase with chamotte. The very low values of V_{ch} are resulted to the very large reduction of the global shrinkage when chamotte is added (Fig. 8a).

The additional porosity from inert grains $V_{add}^{\%}$ is simply the difference between the global porosity of the matrix and the true porosity of the sintered matrix $V_{m}^{\%}$.

$$V_{add}^{\%} = P_{matrix} - V_{m}^{\%} \quad (5)$$

The volume fractions of additional and global porosity in the matrix are presented in Table 4 for the two clays. In general, values of additional porosity increase with the inert grain ratio, i.e. chamotte and quartz in BEAC based material. The high values of additional porosity are also evidenced in Fig. 4a–c photos, where large pores are observed. They are weak zones, which has a strong influence on the global mechanical strength of materials.

4. Conclusion

Refractory clays mixed with chamotte having large grain size are refractory materials with a very heterogeneous microstructure. The sintering behaviour is mostly influenced by the clay matrix behaviour, the chamotte content and the fraction of large quartz grains in the clay matrix. Chamotte and large quartz grains behave as inert phases during sintering and only narrow interactions at the surrounding areas are observed. Particularly, cristobalite is formed onto large quartz grains. During cooling, local stresses occur because of differences in thermal dilatations between different phases. The random repartition of the chamotte and quartz induces a non-uniform sintering behaviour of the matrix. The matrix volume have not an effective contribution to the global sintering process and an additional porosity is formed, with very large pores. Both local cracks from thermal stress and large pores from the additional porosity in the matrix contribute to the weakening of the macroscopic mechanical strength. Nevertheless, characteristics of materials are sufficient for the manufacturing of industrial kilns, used at temperature not exceeding 1200 °C. The variation of dimensions on reheating is very low and ensure the stability and durability of large kilns.

Acknowledgements

The authors acknowledge the financial support from the French Embassy in Cameroon through ‘‘Coopération pour la Recherche Universitaire et Scientifique’’ (CORUS) Project.

References

[1] K. Niihara, New design concept of structural ceramics: ceramics nanocomposites, J. Ceram. Soc. Jpn. 99 (10) (1991) 974–982.
[2] W.H. Tuan, E. Gilbart, R.J. Brook, Sintering of heterogeneous ceramic compact: part 1 Al_2O_3-Al_2O_3, J. Mater. Sci. 24 (1989) 1062–1068.
[3] M. Lalithambika, Fireclay bricks from Kerala clays, Interceramics 6 (1988) 17–19.
[4] L.D. Pilipchatin, Sintering of fire clay kaolin mixtures with refractory clay, Glass Ceram. 57 (5/6) (2000) 212–214.
[5] W.E Lee, Comprehensive Composite Materials, 4, 4.12, Elsevier Science Ltd., 2000, pp. 363–385.
[6] G.W. Brindley, M. Nakahira, The kaolinite-mullite reaction series: I, II, III, J. Am. Ceram. Soc. 42 (1959) 311–323.
[7] M. Dondi, M. Marsigli, I. Venturi, Microstructure and mechanical properties of clay bricks: comparison between fast firing and traditional firing, Br. Ceram. Trans. 98 (1) (1999) 12–18.
[8] C.Y. Chen, G.S. Lan, W.H. Tuan, Microstructural evolution of mullite during the sintering of kaolin powder compacts, Ceram. Int. 26 (7) (2000) 715–720.
[9] U.C. Melo, E. Kamseu, C. Djangang, Effets of fluxes on fired properties between 950–1050 °C of some Cameroonian clays, Tile Bricks Int. 19 (2003) 384–390.
[10] T. Karfa, T.S. Kabre, P. Blanchart, Sintering of a clay from Burkina Faso by dilatometry Influence of the applied load and the pre-sintering heating rate, Ceram. Int. 27 (8) (2001) 875–882.
[11] Ya-Fei Liu, Xing-Qin Liu, Shan-Wen Tao, Guang-Yao Meng, O. Toff Sorensen, Kinetics of the reactive sintering of kaolinite aluminium hydroxide extrudate, Ceram. Int. 28 (5) (2002) 479–486.
[12] M. Hajjaji, S. Kacim, M. Boulmane, Mineralogy and firing characteristics of a clay from the valley of Ourika (Morocco), Appl. Clay Sci. 21 (3/4) (2002) 203–212.
[13] F.A.C. Minlheiro, M.N. Freire, A.G.P. Silva, J.N.F. Holanda, Densification behaviour of red firing Brazilian kaolinitic clay, Ceram. Int. 31 (2005) 757–763.
[14] U.B. Agbarakwe, J.S. Babda, P.J. Masser, Non-uniformities and pores formation, Mater. Sci. Eng. 109 (1989) 9–16.
[15] A. Shui, L. Zeng, K. Uematsu, Relationship between sintering shrinkage anisotropy and particle orientation for alumina powder compacts, Scripta Mater. 55 (9) (2006) 831–834.
[16] I.H. Moon, J.K. LEE, Relation between sinterability and initial packing density in loosely sintered copper sphere compacts, Powder Metall. 30 (4) (1987) 249–254.
[17] G. Aliprandi, Matériaux réfractaires et céramiques techniques, Ed. Septima, Paris, 1996.
[18] G. Lecomte, B. Pateyron, P. Blanchart, Experimental study and simulation of a vertical section mullite-ternary eutectic (985 °C) in the SiO_2–Al_2O_3–K_2O system, Mater. Res. Bull. 39 (10) (2004) 1469–1478.
[19] W.D. Kingery, Introduction to Ceramics, second ed., John Wiley & Sons, 1976.
[20] M.L. Pines, H.A. Bruck, Pressureless sintering of particle-reinforced metal-ceramic composites for functionally grated materials: Part II. Sintering model, Acta Mater. 54 (2006) 1467–1474.